Magnetic circular dichroism of neutral and ionic forms of octaethylhemiporphycene

ARTICLE *in* CHEMICAL PHYSICS · AUGUST 2002

Impact Factor: 1.65 · DOI: 10.1016/S0301-0104(02)00617-1

4 AUTHORS, INCLUDING:

Alexandr Gorski
Instytut Chemii Fizycznej PAN
31 PUBLICATIONS **290** CITATIONS
SEE PROFILE

J. Waluk
Polish Academy of Sciences
257 PUBLICATIONS **3,706** CITATIONS
SEE PROFILE

ELSEVIER

Chemical Physics 282 (2002) 37–49

Chemical Physics

www.elsevier.com/locate/chemphys

Magnetic circular dichroism of neutral and ionic forms of octaethylhemiporphycene

Alexander Gorski[a], Emanuel Vogel[b], Jonathan L. Sessler[c], Jacek Waluk[a,*]

[a] *Institute of Physical Chemistry, Polish Academy of Sciences, Kasprzaka 44, 01-224 Warsaw, Poland*
[b] *Institut für Organische Chemie der Universität, Greinstrasse 4, D-50939 Köln, Germany*
[c] *Department of Chemistry, Institute of Cellular and Molecular Biology, The University of Austin, Austin, TX 77204-5641, USA*

Received 16 January 2002; in final form 15 May 2002

Abstract

Magnetic circular dichroism (MCD) spectra are reported and analyzed for neutral, doubly protonated and doubly deprotonated forms of a recently synthesized porphyrin isomer, 2,3,6,7,11,12,16,17-octaethylhemiporphycene. MCD measurements have allowed the bands corresponding to the Q and Soret electronic transitions in this porphyrin isomer to be separated and assigned. In addition, several higher-lying electronic transitions were located. The absorption and MCD characteristics of the lowest excited electronic states agree well with predictions based on a perimeter model. Hemiporphycene turns out to be a negative-hard chromophore, i.e., the energy separation between two highest occupied molecular orbitals is smaller than the corresponding value for the two lowest unoccupied orbitals. As a consequence, the spectral properties of hemiporphycene are similar to those of another constitutional isomer of porphyrin, the previously studied porphycene. The latter isomer, however, displays a much stronger negative-hard chromophore character than does hemiporphycene, the subject of the present study. The experimental results reported here are corroborated by TD-B3LYP/6-31G** and semiempirical INDO/S calculations of excited electronic states.

1. Introduction

As the result of exploding synthetic interest, a wide range of new porphyrinoids, including reshuffled [1], expanded [2], inverted (also known as N-confused) [3], and contracted [2] porphyrins, have been introduced into the literature in recent years. Among the various properties these systems display or might potentially display, their electronic structure and spectral characteristics are of special interest. This reflects in part the possibility that these compounds could find practical benefit in areas as wide-ranging and diverse as medicine [4] (phototherapeutic or photodiagnostic substances), material science [5] (sensors, light-emitting devices, solar cells) and information storage [6] (optical memories, photoswitches). Reshuffled porphyrins, or, more precisely, constitutional isomers of porphyrin, are very promising in all these areas. Following the synthesis of porphycene [7] (porphyrin-(2.0.2.0)), the first "nitrogen-in"

* Corresponding author. Tel.: +4822-632-7269; fax: +48-391-20-238.
E-mail address: waluk@ichf.edu.pl (J. Waluk).

0301-0104/02/$ - see front matter
PII: S0301-0104(02)00617-1

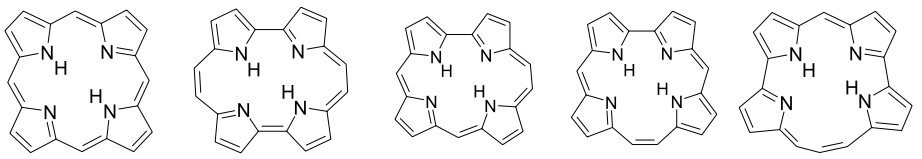

Chart 1. Left to right: porphyrin, porphycene; hemiporphycene, corrphycene and isoporphycene.

isomer of the parent porphyrin (porphyrin-(1.1.1.1)), three more members of the group have been produced (as alkylated derivatives) in the last decade: hemiporphycene [8] (porphyrin-(2.1.1.0)), corrphycene [9] (porphyrin-(2.1.0.1)) and isoporphycene [10] (porphyrin-(3.0.1.0)) (Chart 1). The (*k.l.m.n*) notation refers to the number of *meso*-like bridging carbon atoms linking the individual pyrrolic subunits. Three isomers, porphyrin-(2.2.0.0), -(3.1.0.0) and -(4.0.0.0) have not yet been synthesized. However, theoretical studies have been carried out for all the members of the class. These investigations included calculations of relative stabilities, geometries, tautomeric equilibria, as well as predictions of spectral and electronic properties [11–15]. The latter were also the subject of a theoretical analysis based on a simple perimeter model [11,16,17]. This procedure led to predictions regarding the electronic absorption and magnetic circular dichroism (MCD) spectra. At the time of this study, the only isomer available was porphycene. Its spectral properties were shown to agree well with the results of theoretical analysis, in particular those regarding the absorption and MCD patterns [18]. The availability of new isomers now makes it possible to verify the theoretical predictions for related compounds. In this work we examine the electronic absorption and MCD spectra of neutral, doubly deprotonated, and doubly protonated 2,3,6,7,11,12,16,17-octaethylhemiporphycene (**1**, see Chart 2). It is demonstrated that the experimentally observed spectral features and trends are well accounted for by an analysis based on a perimeter model. Using the nomenclature of this model [16,17], hemiporhycene acts as a ''negative hard'' chromophore and displays analogy to porphycene. In a separate paper, we analyse the MCD spectroscopy of another constitutional isomer of porphyrin, namely 2,3,6,7,11,12,17,18-octaethylcorrphycene, which,

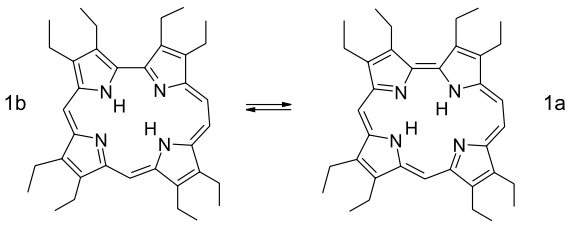

Chart 2. The *trans* tautomeric forms of 2,3,6,7,11,12,17,18-octaethylhemiporrphycene (**1**).

like porphyrin itself, turns out to be a much ''softer'' chromophore [19].

2. Experimental and computational details

The synthesis and purification of **1** have been described elsewhere [8]. Spectral grade solvents were used for the preparation of solutions of **1**. The spectra of the neutral species were measured in acetonitrile solution. The doubly protonated form was produced by adding excess perchloric acid to an acetonitrile solution, while the dianion was made and studied in dimethylsulfoxide (DMSO), saturated with KOH. Absorption spectra were measured on a Shimadzu UV3100 spectrophotometer. MCD spectra were recorded on a JASCO J-715 spectropolarimeter, equipped with two different home-built magnets: (i) a permanent magnet (field strength 2.9 kG); (ii) an electromagnet (field intensity variable in the range 0–5 kG). In order to enhance the MCD signal and to minimize the baseline artifacts, the MCD spectra were obtained as the difference between the curves recorded with the opposite directions of the magnetic field. The values of the Faraday *B* terms were extracted from the spectra using the method of moments, by integrating the bands measured in isotropic solution:

$$B = -33.53^{-1} \int \mathrm{d}\tilde{\nu}[\Theta]_{\mathrm{M}}/\tilde{\nu}, \quad (1)$$

where $[\Theta]_{\mathrm{M}}$ is the magnetically induced molar ellipticity per unit magnetic field (in units of deg L m^{-1} mol^{-1} G^{-1}), and $\tilde{\nu}$ is the wavenumber.

Excited state energies, oscillator strengths, and the transition polarizations were calculated for parent non-alkylated structures using the TD-B3LYP method with the 6-31G** basis set, as implemented in the GAUSSIAN 98 program package [20]. Prior to these time-dependent density functional theory (DFT) excited state energy calculations, the geometry of each form was optimized by the B3LYP/6-31G** method. To ensure that the structures obtained in this way correspond to real minima, the results were checked for the absence of negative frequencies. For calculations of alkylated derivatives, we employed the INDO/S method [21], which, in addition to yielding the quantities computed by TD-DFT, allowed us to calculate the values of the MCD B terms. Finally, AM1 [22] and PM3 [23] procedures were used to calculate the ground state structure and orbital splittings in both parent and alkyl-substituted compounds.

3. Results and discussion

The experimentally observed spectral features are presented in Table 1 for the neutral, doubly

Table 1
Experimentally determined absorption and MCD characteristics for neutral, doubly protonated and doubly deprotonated 2,3,6,7,11,12,16,17-octaethylhemiporphycene

	Absorption		MCD		Assignment
	$\tilde{\nu}$[a]	ε	$\tilde{\nu}$[a]	B[b]	
Neutral form[c]	15.9	9,700	15.8	−8.6	L_1
	17.2	7,600	16.9	15.4[f]	L_2
	18.2	24,000	18.1		
	19.7	6,800	19.5		
			23.9	5.5	B_1
	24.9	144,700	24.8	−5.7	B_2
			26.1	12.0	
			31.2	6.7	
			39.4	4.1	
Doubly protonated form[d]	16.1	17,000	16.1	−25.7	L_1
	16.8	16,000	16.7	32.5	L_2
	17.7	4,900			
	18.2	5,100			
			23.7	10.1	B_1
	24.3	212,000	24.5	−4.7	B_2
			26.1	6.1	
			28.6	5.4	
Doubly deprotonated form[e]	16.1	48,000	15.8	−44.8	L_1
			16.1	55.7	L_2
	17.2	10,000			
	23.4	160,000	23.3	−6.3	B_1
			25.3	8.0	B_2
			28.9	4.9	

[a] 10^3 cm^{-1}.
[b] Faraday B terms $[D^2\mu_B/cm^{-1}]$.
[c] Room temperature acetonitrile solution of **1**, with the **1a**:**1b** ratio of about 7:3 [25].
[d] Room temperature solution of **1** in acetonitrile containing perchloric acid.
[e] Room temperature solution of **1** in KOH-saturated dimethylsulfoxide.
[f] Obtained from integration of negative bands at 16,900 and 18,100 cm^{-1}.

protonated and doubly deprotonated forms of **1**. Figs. 1–3 show the absorption and MCD spectra. Included in the figures are also the INDO/S theoretical predictions regarding the transition energies and MCD *B* terms, as well as the TD-DFT values of excited state energies of the neutral and charged forms, calculated for the unsubstituted hemiporphycene. The results of the TD-DFT calculations are presented in more detail in Tables 2–5.

The absorption spectra of **1** reveal a pattern characteristic of porphyrin and its derivatives, namely weak bands in the low-energy range (Q-region), followed at higher energies by an intense band (Soret region). The Q/Soret intensity ratio is significantly larger than in porphyrin, but smaller than in porphycene [18]. The MCD spectra clearly show the presence of two electronic transitions in

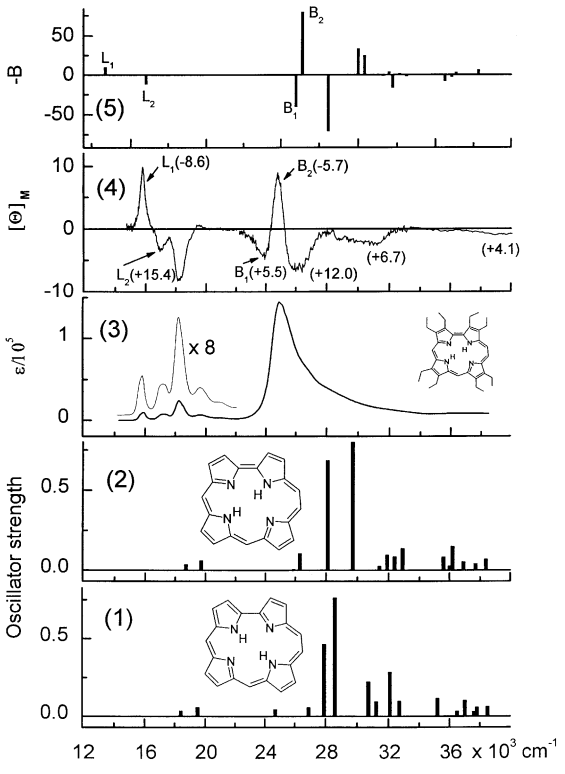

Fig. 1. From bottom to top: (1) and (2) TD-DFT calculated electronic transitions for two tautomeric forms of the parent unsubstituted hemiporphycene; electronic absorption (3) and MCD (4) spectra of neutral **1** (*B* term values ($D^2\mu_B/cm^{-1}$) in parentheses); (5) the results of INDO/S calculations for **1a**. The calculated values of *B* terms are indicated by the bars. The spectra were recorded in acetonitrile at 293 K.

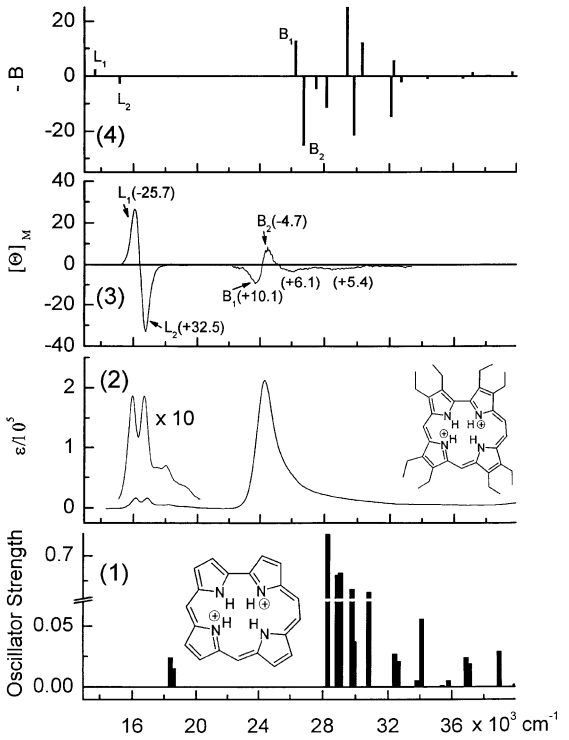

Fig. 2. (1) TD-DFT calculated electronic transitions for the dication of the parent unsubstituted hemiporphycene; electronic absorption (2) and MCD (3) spectra of doubly protonated **1**; (4) the results of INDO/S calculations for the doubly protonated form of **1**. The spectra were recorded in acetonitrile solution containing perchloric acid at 293 K. See caption to Fig. 1 for details.

the Q region, with the same −, + sign pattern for all forms (it should be recalled that a positive MCD sign corresponds to a negative value of the *B* term, and vice versa). In the Soret region, for the neutral and doubly protonated forms the MCD curves reveal the presence of an additional electronic transition, located to the blue of the two Soret bands. Other electronic transitions are detected at somewhat higher energies; for the dianion, one of them is seen as a separate band in the absorption spectrum, while the corresponding transitions are buried in the high energy tail of the main Soret band in the case of the other forms.

Before analyzing the spectra using the perimeter model [16,17], we briefly recall its main features as they relate to the present case. The basic hemiporphycene chromophore can be derived formally

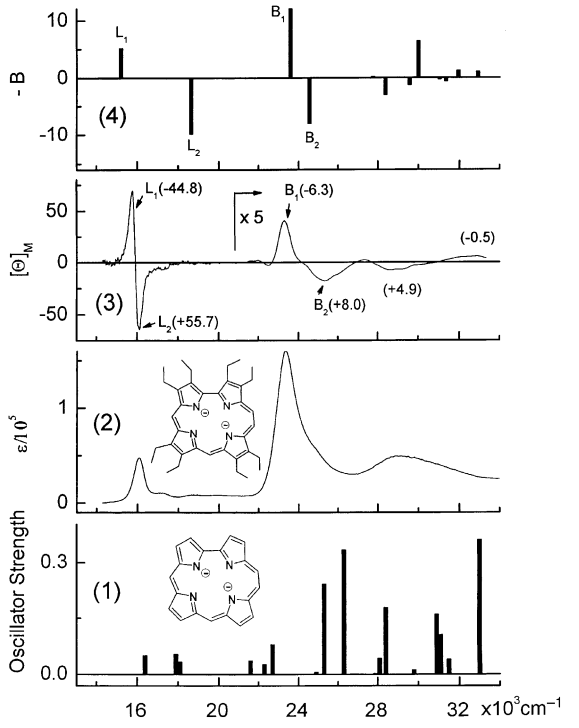

Fig. 3. (1) TD-DFT calculated electronic transitions for the dianion of the parent unsubstituted hemiporphycene; electronic absorption (2) and MCD (3) spectra of doubly deprotonated **1**; (4) the results of INDO/S calculations for the doubly deprotonated form of **1**. The spectra were recorded in a KOH-saturated DMSO solution at 293 K. See caption to Fig. 1 for details.

from a perimeter containing 18 π electrons – the [20]annulene dication, $C_{20}H_{20}^{2+}$, by bridging with two –NH– groups at positions 1–4 and 10–13 and with two $-N^{-}-$ groups at positions 5–8 and 15–18 (Fig. 4). The choice of a doubly positively charged 18-electron [20]annulene as a starting point is dictated by the fact that charged $4N+2$ perimeters have a degenerate pair of low lying L_1 and L_2 states, whereas another possible selection – a neutral [18]annulene – exhibits a large splitting between these states. Since the L_1 and L_2 states lie very close in porphyrin, and even closer in porphycene [18] and, as it turns out, in hemiporphycene **1**, a derivation starting from a charged [20]annulene perimeter represents a much smaller perturbation than the alternative case of starting from an uncharged [18]annulene.

The electronic states considered in the present study are those derived from four singly excited configurations corresponding to excitations from the two highest occupied (HOMO) π-orbitals into the two lowest unoccupied (LUMO) π-orbitals. Configuration interaction produces four states, labeled L_1, L_2, B_1 and B_2 in the order of increasing energy. In porphyrin and its derivatives, the two lower transitions are usually referred to as Q bands, while the two higher ones are known as Soret bands. The degree of the mixing of the L states with the B states can be expressed by the values of the parameters α and β, which, in turn, are simple functions of the splittings of the initially degenerate HOMO and LUMO pairs:

$$\tan(2\alpha) = 2(|a| + |b|)/[E(\mathrm{B}) - E(\mathrm{L})], \tag{2}$$

$$\tan(2\beta) = 2(|a| - |b|)/[E(\mathrm{B}) - E(\mathrm{L})], \tag{3}$$

$$\Delta\mathrm{HOMO} = 2|a|, \tag{4}$$

$$\Delta\mathrm{LUMO} = 2|b|. \tag{5}$$

$E(\mathrm{B}) - E(\mathrm{L})$ is the energy difference between the L and B states in the parent perimeter; a and b are the complex parameters that describe the perturbation that leads to the splitting of HOMO and LUMO, respectively. Using these parameters, explicit expressions can be obtained for the transition dipole strengths and polarizations, as well as for the values of the MCD terms [16–18]. In the present paper, we focus on the latter. Assuming that ΔL, the energy separation between the two L states, and ΔB, the separation between the two B states are much smaller than the L–B spacing, one obtains the following equations:

$$B(\mathrm{L}_1) = -B(\mathrm{L}_2) = -[m^2/(2\Delta\mathrm{L})] \times (4\mu^{-}\sin^2\alpha\sin^2\beta + \mu^{+}\sin 2\alpha\sin 2\beta), \tag{6}$$

$$B(\mathrm{B}_1) = -B(\mathrm{B}_2) = -[m^2/(2\Delta\mathrm{B})] \times (4\mu^{-}\cos^2\alpha\cos^2\beta + \mu^{+}\sin 2\alpha\sin 2\beta). \tag{7}$$

The quantity m, the electric transition dipole contribution, is a simple function of N and of the perimeter size, n. Similarly, the magnetic moment contributions μ^{+} and μ^{-} also depend on N and n. The μ^{+} contributions are negative and about a magnitude larger than the μ^{-} terms, usually also negative.

Table 2
Calculated (TD-B3LYP/6-31G**) electronic states of the tautomer **1a** of neutral parent hemiporphycene

	Calc. energy[a] (10^3 cm^{-1})	Oscillator strength	Dominant configuration[b]
1	18.7	0.037	0.57 (1 −1)
2	19.7	0.061	0.55 (2 −1)
3	25.9	0.006	0.67 (3 −1)
4	26.3	0.106	0.57 (4 −1)
5	28.1	0.684	0.46 (1 −2)
6	29.7	0.801	0.36 (2 −2)
7	31.2	0.000	0.64 (7 −1)
8	31.4	0.026	0.59 (5 −1)
9	31.4	0.000	0.64 (6 −1)
10	31.9	0.095	0.59 (3 −2)
11	32.4	0.085	0.67 (4 −2)
12	32.9	0.136	0.66 (6 −1)
13	35.6	0.083	0.44 (9 −1), 0.43 (2 −2)
14	36.0	0.027	0.44 (6 −2), 0.41 (5 −2)
15	36.2	0.001	0.69 (7 −2)
16	36.2	0.150	0.57 (1 −3)
17	36.4	0.001	0.69 (8 −2)
18	36.9	0.053	0.49 (6 −2)
19	37.7	0.041	0.46 (10 −1)
20	38.4	0.069	0.40 (2 −3)

[a] Calculated for the unsubstituted molecule.
[b] The occupied orbitals are numbered $1, 2, \ldots$ downwards, the unoccupied ones, $-1, -2, \ldots$ upwards.

Table 3
Calculated (TD-B3LYP/6-31G**) electronic states of the tautomer **1b** of neutral parent hemiporphycene

	Calc. energy (10^3 cm^{-1})	Oscillator strength	Dominant configuration
1	18.4	0.035	0.55 (2 −1)
2	19.5	0.057	0.55 (1 −1)
3	24.7	0.045	0.61 (3 −1)
4	26.9	0.056	0.62 (4 −1)
5	27.9	0.465	0.33 (4 −1), 0.32 (1 −2)
6	28.6	0.763	0.46 (2 −2)
7	30.7	0.222	0.50 (4 −2)
8	31.0	0.000	0.69 (6 −1)
9	31.2	0.093	0.57 (3 −2)
10	32.0	0.000	0.70 (8 −1)
11	32.1	0.285	0.55 (5 −1)
12	32.7	0.096	0.65 (6 −1)
13	34.6	0.000	0.68 (7 −2)
14	35.2	0.116	0.52 (1 −3)
15	36.5	0.034	0.55 (2 −3)
16	36.7	0.001	0.67 (8 −2)
17	37.0	0.102	0.61 (5 −2)
18	37.6	0.030	0.45 (6 −2)
19	37.8	0.058	0.42 (10 −1)
20	38.5	0.063	0.49 (6 −2)

See captions to Table 2 for details.

Table 4
Calculated (TD-B3LYP/6-31G**) electronic states of the doubly protonated form of parent hemiporphycene

	Calc. energy (10^3 cm^{-1})	Oscillator strength	Dominant configuration
1	18.4	0.024	0.48 (1 −1)
2	18.6	0.015	0.43 (1 −2)
3	28.3	0.989	0.41 (1 −2)
4	28.9	0.429	0.52 (3 −1)
5	29.1	0.460	0.43 (3 −1)
6	29.8	0.232	0.57 (5 −1)
7	29.9	0.037	0.64 (6 −1)
8	30.8	0.193	0.59 (4 −1)
9	32.4	0.027	0.65 (4 −2)
10	32.6	0.021	0.67 (3 −2)
11	33.8	0.005	0.64 (5 −2)
12	34.1	0.056	0.67 (6 −2)
13	35.4	0.001	0.54 (7 −1)
14	35.8	0.005	0.50 (8 −1)
15	36.9	0.024	0.42 (7 −2)
16	37.1	0.019	0.38 (1 −3)
17	39.0	0.029	0.39 (1 −4)
18	40.0	0.002	0.50 (8 −2)
19	44.1	0.031	0.30 (1 −4)
20	44.8	0.005	0.61 (9 −1)

See captions to Table 2 for details.

Table 5
Calculated (TD-B3LYP/6-31G**) electronic states of the parent hemiporphycene dianion

	Calc. energy (10^3 cm^{-1})	Oscillator strength	Dominant configuration
1	16.4	0.051	0.49 (1 −1)
2	17.9	0.054	0.41 (1 −2)
3	18.1	0.034	0.56 (3 −1)
4	21.6	0.037	0.44 (4 −1)
5	22.7	0.079	0.42 (4 −1), 0.38 (5 −1)
6	22.3	0.027	0.46 (3 −2)
7	24.9	0.006	0.65 (6 −1)
8	25.3	0.242	0.41 (4 −1)
9	26.3	0.334	0.45 (2 −2)
10	27.9	0.003	0.60 (4 −2)
11	28.1	0.043	0.58 (8 −1)
12	28.4	0.179	0.48 (7 −1)
13	29.8	0.012	0.52 (6 −2)
14	30.9	0.160	0.58 (5 −2)
15	31.1	0.105	0.53 (9 −1)
16	31.3	0.001	0.47 (10 −1)
17	31.5	0.040	0.51 (6 −2), 0.36 (1 −3)
18	3.0	0.360	0.48 (1 −3)
19	34.3	0.005	0.67 (7 −2)
20	35.1	0.222	0.55 (2 −4)

See captions to Table 2 for details.

Formulas (6) and (7) show that the crucial quantity that determines the sign of the MCD *B* terms is the parameter β, which can be approximated as $(\Delta\mathrm{HOMO} - \Delta\mathrm{LUMO})/\{2[E(\mathrm{B}) - E(\mathrm{L})]\}$. Thus, when the difference $\Delta\mathrm{HOMO} - \Delta\mathrm{LUMO}$ is positive, a sequence of $+, -, +, -$ signs

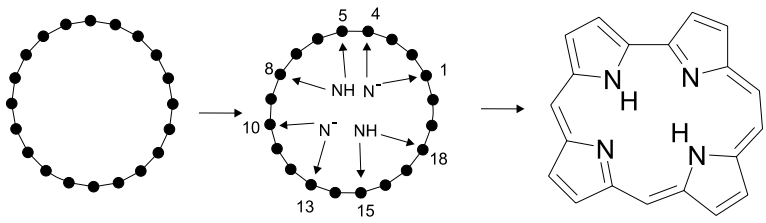

Fig. 4. Formal derivation of hemiporphycene from an 18 π electron perimeter, the [20]annulene dication ($C_{20}H_{20}^{2+}$).

of the *B* terms for the L_1, L_2, B_1 and B_2 transitions is expected. For a negative value of $\Delta HOMO - \Delta LUMO$, a $-,+,+,-$ sequence is expected for weak perturbations, since in this case the sign of the *B* terms for B transitions is dictated by contributions from μ^-. For larger perturbations, the μ^+ terms will dominate, and the sequence of *B* terms will change to $-,+,-,+$. The border between the "weak" and "strong" perturbation can be expressed in terms of the ratio of dipole strengths of the L and B transitions. It was estimated that for a $C_{20}H_{20}^{2+}$ macrocyclic periphery this border or limit corresponds to $D(L)/D(B) \approx 0.1$ [18]. The interplay between the μ^+ and μ^- contributions was experimentally observed for various forms of porphycene; here the sign of $B(B_1)$ was positive for the species corresponding to a less perturbed perimeter, such as N-protonated porphycene, while for stronger perturbations (neutral and dianionic forms) the $B(B_1)$ sign was found to be negative [18].

Chromophores with large values of $|\Delta HOMO - \Delta LUMO|$ are unlikely to change their MCD signs, even after significant perturbations, and have therefore been referred to as "hard": positive-hard for $\Delta HOMO > \Delta LUMO$ and negative-hard for $\Delta HOMO < \Delta LUMO$ ("positive" and "negative" refer to the expected sign of $B(L_1)$). By contrast, "soft" chromophores are characterized by $\Delta HOMO \approx \Delta LUMO$, meaning even a weak perturbation, such as, e.g., substitution by an alkyl group can dictate the MCD signs.

The beauty and usefulness of the perimeter model lies in the fact that it allows to predict the character of a chromophore on the basis of simple orbital considerations. Fig. 5 shows the predicted response of the frontier orbitals of $C_{20}H_{20}^{2+}$ perimeter to bridging in accord with the structural perturbations required to produce hemiporphycene. The amount by which an orbital of the parent $C_{20}H_{20}^{2+}$ perimeter will be destabilized depends on the values of LCAO coefficients at the bridging position. Moreover, no change in orbital energy is expected if the –NH– or $-N^-$– groups lie in the nodal plane. Taking this into consideration, it can be concluded that the bridging perturbations needed to produce hemiporphycene should not affect substantially the two HOMO orbitals. In contrast, the two components of the LUMO pair should be destabilized, each to a different degree: one of the orbitals is expected to interact with three of the bridges, while the energy of the other is pushed upwards by only one bridge. Thus, the expected splitting of the LUMO pair should be larger than that of the HOMO pair, leading to $\Delta HOMO < \Delta LUMO$ and thus, to a negative-hard chromophore. (It should be recalled that in porphycene, all four bridges raise the energy of one LUMO orbital, leaving the other unchanged [11]; this is predicted to lead to a larger splitting than in hemiporphycene). Since the $-N^-$– group induces a greater perturbation than a corresponding –NH– bridge, the LUMO splitting should be the largest in the dianion, and the smallest in the doubly protonated form of hemiporphycene. For the latter, additional spectroscopically observable effects could arise from the presumed non-planarity. However, our results show that these secondary considerations are not important. It has been established that the neutral forms consists of two *trans* tautomers (**1a** and **1b** in Chart 2), of which the former is more stable by about 1 kcal/mol [24,25]. The electronic spectra of the two tautomers are very similar: in a polar solvent, the spectra overlap to such a degree that it is not possible to distinguish features due to a particular tautomeric form. The same is true for MCD spectra, which confirms that the orbital splitting pattern should be qualitatively the

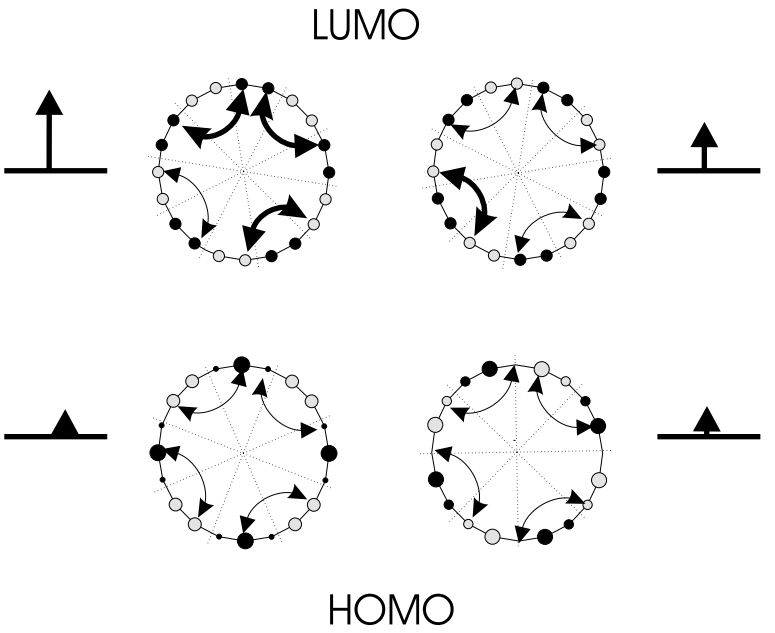

Fig. 5. The shapes of the HOMO and LUMO orbitals of the parent $C_{20}H_{20}^{2+}$ perimeter and the expected energy shifts caused by the perturbations corresponding to the formation of hemiporphycene.

same for both tautomers, with only minor differences in the orbital splitting values. Actually, in the case of a tautomeric equilibrium occurring in a soft chromophore, the situation would have been much different: different signs of $\Delta\mathrm{HOMO} - \Delta\mathrm{LUMO}$ and thus, different MCD signs could be expected for the different tautomers, as has been discussed previously for porphyrin and its derivatives [26].

In a decade-old paper devoted to theoretical analysis of various "nitrogen-in" constitutional isomers of porphyrin, we calculated the orbital splittings using the PPP method [11]. The present results are qualitatively the same and quantitatively not much different. The values of ΔHOMO computed using B3LYP/6-31G** are 0.08, 0.04, 0.11, and 0.32 eV for the dication, tautomer **1a**, tautomer **1b**, and the dianion, respectively. The corresponding ΔLUMO values are 0.39, 0.57, 0.57, and 0.66 eV. The inequality $\Delta\mathrm{HOMO} < \Delta\mathrm{LUMO}$ is obtained no matter which theoretical method is used. This leads us to suggest that even simple theoretical analyses will prove satisfactory in terms of predicting the "hard" character of a chromophore. Naturally, for "soft" or nearly "soft" chromophores, the situation is more complicated, and the exact determination of the sign of $\Delta\mathrm{HOMO} < \Delta\mathrm{LUMO}$ is expected to require more sophisticated approaches.

The above orbital splitting values were obtained for parent, unsubstituted molecules. As can be concluded from the inspection of the shape of molecular orbitals of the parent perimeter in hemiporphycene (Fig. 5), substitution by eight alkyl groups should not have much influence on the splitting pattern. We checked this prediction by comparing the results of AM1 and PM3 calculations performed both for the unsubstituted and octamethyl-substituted species. Qualitatively similar results were obtained in both cases.

Having established the negative-hard character of the hemiporphycene chromophore ($\beta < 0$), we now can make predictions regarding signs and intensities in its absorption and MCD spectra. For the Q-bands region, this is easy. The expected $-,+$ sequence of the signs of B terms for the L_1 and L_2 transitions is unequivocal, since the μ^+ contributions dominate (cf. Eq. (6)). Theory thus predicts that the MCD intensities should be strongest for the dianionic forms, which correspond to the largest perturbation of the parent perimeter. Moreover, due to the nature of L–B magnetic

mixing, the absolute values of $B(L_2)$ should be larger than those of $B(L_1)$. All these predictions are confirmed by experiment as seen in Figs. 1–3.

In the region of the Soret bands (B states), the analysis is more challenging. Now, the μ^+ contributions will be dominant only in the case of a sufficiently strong perturbation (Eq. (7)). We noted above that borderline behavior was observed in porphycene, where a $+,-$ pattern, observed for the dication changes into $-,+$ in the neutral and doubly deprotonated forms [18]. The inequality $\Delta\mathrm{HOMO} < \Delta\mathrm{LUMO}$ is stronger in the case of porphycene than in hemiporphycene. We may thus expect that the perturbation of the perimeter occurring upon formation of hemiporphycene may not be strong enough to make the μ^+ term dominant in the formulas that allow for predictions of $B(B)$. For such case, a $+,-$ sequence is predicted for $B(B_1)$ and $B(B_2)$. Figs. 1–3 show that such behavior is observed in the dication and neutral **1**. However, in the dianion the pattern changes to $-,+$. This result proves again that porphycene is a stronger "negative-hard" chromophore than hemiporphycene: in the latter, only the strongest perturbation of the perimeter (bridging by four –N^-– groups) is able to reverse the $B(B_1), B(B_2)$ sign pattern, whereas for porphycene, this effect is already observed for a weaker perturbation, bridging by two –NH– and two –N^-– groups. These theoretical considerations also lead to the prediction that, as a consequence of L–B magnetic mixing, the magnitude of the B term for B_1 should be smaller than for B_2. This is clearly observed for the dianionic form; in the neutral and protonated species, some cancellation of the MCD intensity in the region of B_2 occurs, due to overlap with another close-lying higher energy transition.

The perimeter model also allows predictions regarding intensities of the individual bands in the absorption spectra of the dicationic, neutral and dianionic forms of hemiporphycene. In the case of strongly overlapping L_1–L_2 and B_1–B_2 pairs of transitions, it is difficult to assess the intensities of the individual components. Instead, it is better to use the sums of dipole strengths for the L (Q) and B (Soret) bands. The intensity ratio $D(L)/D(B) = [D(L_1) + D(L_2)]/[D(B_1) + D(B_2)]$ should increase with growing strength of the perturbation. Indeed, the experimentally observed ratio is largest for the dianionic form, smaller for the neutral form, and the smallest in the dication (although, due to the presence of an additional band in the Soret region, this trend can only be expressed qualitatively). The following equation relates the intensity ratio to the values of orbital splittings [18]:

$$D(L)/D(B) = (-1/4)[\Delta\mathrm{HOMO}^2 - \Delta\mathrm{LUMO}^2] / [E(B) - E(L)]^2. \quad (8)$$

Inserting the B3LYP/6-31G** calculated values of orbital splittings into Eq. (8) leads to the prediction that the $D(L)/D(B)$ ratio will increase in the order: dication, neutral, and dianion, exactly as observed.

The above results demonstrate the usefulness and reliability of a simple perimeter model when predicting the absorption and MCD spectral patterns. One can expect that the accuracy of this approach will depend on how well an excited state can be defined in terms of four configurations only. In particular, the validity of this model could be called into question with regard to the Soret transitions, since here experiment shows a presence of at least one nearby electronic state.

A good measure of the accuracy of description of a given state by a perimeter model (or, for that matter, by a closely related four-orbital model of Gouterman [27]) is provided by the value of the sum of the squares of the four CI coefficients that describe the four configurations of the perimeter model. We have recently computed values for this parameter, performing a series of calculations that used various sizes of CI bases for porphyrin [28], porphycene [28], dibenzoporphycenes [28], octaethylcorrphycene [19], and smaragdyrins [29]. The better the description by the four-orbital model is, the closer the value will approach unity for a given electronic state.

The INDO/S calculated values for two tautomers of **1** and its charged forms are shown in Table 6. It can be seen that the L states, i.e. those leading to the Q bands, are always described perfectly in terms of the four-orbital model. For the Soret transitions, the model works well for charged species, while in neutral forms one of the states is mixed with other electronic transitions. A

Table 6
Values of the sums of squares of the four CI coefficients describing the contributions from the single excitations considered in the four-orbital model

	1a		1b		Dication		Dianion	
L_1	15.4 (0.03)	0.96	13.4 (0.04)	0.95	13.6 (0.06)	0.97	15.2 (0.20)	0.93
L_2	16.3 (0.15)	0.97	16.0 (0.07)	0.98	15.2 (0.00)	0.97	18.6 (0.05)	0.95
B_1	27.9 (1.49)	0.55	26.0 (0.77)	0.38	26.3 (2.35)	0.70	23.6 (1.08)	0.92
B_2	27.8 (1.68)	0.79	26.4 (1.64)	0.73	26.8 (2.21)	0.75	24.6 (0.81)	0.87
			28.1 (1.13)	0.35				

These values were extracted from calculations that used 196 (14×14) singly excited configurations.

similar situation was encountered when the same computational approach was applied to the parent system, porphyrin [28], and to octaethylcorrphycene [19].

The values of transition energies and oscillator strengths, calculated using TD-DFT for the unsubstituted form of hemiporphycene, are shown in Figs. 1–3 and Tables 2–5 and compared with the experimental results obtained for the alkylated molecule. The experimental and calculated values are in quite good agreement. The calculations overestimate the transition energies by 0.1–0.4 eV, a result similar to what was found for free base and metalloporphyrin derivatives using TD-DFT and various ab initio schemes [30]. In fact, the agreement would have been much better if the alkyl substituents were included in the calculations. For magnesium porphyrin, it has been reported that the TD-DFT calculated values for tetramethyl–tetraethyl-substituted molecule are lower by 0.2–0.3 eV than the values obtained for the unsubstituted molecule [30]. On the other hand, much better agreement is obtained for the splitting between the L and B pairs in **1**. Moreover, the calculations correctly predict that for the neutral species the lowest excited singlet state of tautomer **1a** lies higher than in form **1b**, and that for the second excited state this ordering is reversed.

4. Summary and conclusions

Our work has allowed to locate the L and B transitions and several higher electronic states in the doubly protonated and doubly deprotonated forms of 2,3,6,7,11,12,16,17-octaethylhemiporphycene, **1**. An analysis of the MCD spectra based on a perimeter model makes it possible to understand the pattern of the signs and intensities, as well as the trends observed within the series of the constitutional isomers, consisting of porphyrin, porphycene, corrphycene, and hemiporphycene. Spectral properties place hemiporphycene alongside porphycene, a negative-hard chromophore. In a separate work [19], we report that corrphycene, another recently synthesized porphyrin isomer, occupies a position close to porphyrin, a soft chromophore.

The negative-hard character of the hemiporphycene chromophore implies a relatively strong absorption in the visible region and thus forebodes possible applications of this particular system as a sensitizer in photodynamic therapy. On the other hand, it has been established that other conditions required for a success in this particular application area, namely good triplet state and singlet oxygen formation efficiencies, are met for the neutral form of **1** [8]. Thus, simple theoretical analyses along the lines presented here could serve as the starting point for the design of new compounds with more desirable spectral properties. In particular, strong negative-hard character, and thus intense absorption bands in the visible region, should be expected for porphyrin-(2.2.0.0) and porphyrin-(4.0.0.0), as well as for the pentapyrrolic system, pentaphyrin-(0.0.0.0.0) [11]. These molecules remain yet to be synthesized.

Acknowledgements

We are grateful to Prof. J. Michl and Dr. J. Downing (University of Colorado, Boulder) for allowing us to use their version of the INDO/S

program. We thank Prof. J. Frelek from the Institute of Organic Chemistry of the Polish Academy of Sciences for allowing us to use the JASCO spectropolarimeter. The work was sponsored, in part, by the KBN grants 3T09A 063 14 and 7T09A 02420. Support to J.L.S. under the terms of NSF grant CHE 9725399 is also gratefully acknowledged. Some of the results of this work were obtained using the computer resources of the Interdisciplinary Centre for Mathematical and Computational Modelling (ICM) of the Warsaw University.

References

[1] J.L. Sessler, A. Gebauer, E. Vogel, in: K.M. Kadish, K.M. Smith, R. Guillard (Eds.), The Porphyrin Handbook, vol. 2, Academic Press, San Diego, 2000 (Chapter 8).
[2] (a) J.L. Sessler, A. Gebauer, S.J. Weghorn, in: K.M. Kadish, K.M. Smith, R. Guillard (Eds.), The Porphyrin Handbook, vol. 2, Academic Press, San Diego, 2000 (Chapter 9);
(b) J.L. Sessler, S.J. Weghorn, Expanded, Contracted and Isomeric Porphyrins, Organic Chemistry Series, vol. 15, Pergamon, New York, 1997.
[3] L. Latos-Grażyński, in: K.M. Kadish, K.M. Smith, R. Guillard (Eds.), The Porphyrin Handbook, vol. 2, Academic Press, San Diego, 2000 (Chapter 14).
[4] (a) R. Bonnet, Chem. Soc. Rev. (1995) 19;
(b) J. Fuchs, S. Weber, R. Kaufmann, Free Rad. Biol. Med. 28 (2000) 537.
[5] (a) K. Ariga, K. Endo, Y. Aoyama, Y. Okahata, Colloids Surf. A 169 (2000) 177;
(b) A. Chowdhury, A.J. Pal, Thin Solid Films 385 (2001) 266;
(c) T. Akiyama, A. Miyazaki, M. Sutoh, I. Ichonose, T. Kunitake, S. Yamada, Colloids Surf. A 169 (2000) 137.
[6] (a) D.R. Reddy, B.G. Maiya, Chem. Commun. (2001) 117;
(b) J. Otsuki, K. Harada, K. Araki, Chem. Lett. 3 (1999) 269;
(c) S. Tsuchiya, J. Am. Chem. Soc. 121 (1999) 48;
(d) K.H. Neumann, F.J. Vogtle, Chem. Soc. Chem. Comm. (1988) 520;
(e) M. Drobizhev, C. Sigel, A. Rebane, J. Luminescence 86 (2000) 391.
[7] E. Vogel, M. Köcher, H. Schmickler, J. Lex, Angew. Chem. Int. Ed. Engl. 25 (1986) 257.
[8] (a) H.J. Callot, A. Rohrer, T. Tschamber, B. Metz, New. J. Chem. 19 (1995) 155;
(b) E. Vogel, M. Bröring, S.J. Weghorn, P. Scholz, R. Deponte, J. Lex, H. Schmickler, K. Schaffner, S.E. Braslavsky, M. Müller, S. Pörting, C.J. Fowler, J.L. Sessler, Angew. Chem. Int. Ed. Engl. 36 (1997) 1651.
[9] J.L. Sessler, E.A. Brucker, S.J. Weghorn, M. Kisters, M. Schäfer, J. Lex, E. Vogel, Angew. Chem. Int. Ed. Engl. 33 (1994) 2308.
[10] (a) E. Vogel, M. Bröring, C. Erben, R. Demuth, J. Lex, M. Nendel, K.N. Houk, Angew. Chem. Int. Ed. Engl. 36 (1997) 353;
(b) E. Vogel, P. Scholz, R. Demuth, C. Erben, M. Bröring, H. Schmickler, J. Lex, G. Hohlneicher, D. Bremm, Y.-D. Wu, Angew. Chem. Int. Ed. Engl. 38 (1999) 2919.
[11] J. Waluk, J. Michl, J. Org. Chem. 56 (1991) 2729.
[12] Z. Hu, J.L. Atwood, M.P. Cava, J. Org. Chem. 59 (1994) 8071.
[13] E. Vogel, M. Broring, J. Fink, D. Rosen, H. Schmickler, J. Lex, K.W.K. Chan, Y.-D. Wu, D.A. Plattner, M. Nendel, K.N. Houk, Angew. Chem. Int. Ed. Engl. 34 (1995) 2511.
[14] Y.-D. Wu, K.W.K. Chan, C.-P. Yip, E. Vogel, D.A. Plattner, K.N. Houk, J. Org. Chem. 62 (1997) 9240.
[15] A. Ghosh, K. Jynge, J. Phys. Chem. B 101 (1997) 5459.
[16] (a) J. Michl, J. Am. Chem. Soc. 100 (1978) 6801;
(b) J. Michl, J. Am. Chem. Soc. 100 (1978) 6812;
(c) J. Michl, J. Am. Chem. Soc. 100 (1978) 6819.
[17] J. Michl, Tetrahedron 40 (1984) 3845.
[18] J. Waluk, M. Müller, P. Swiderek, M. Köcher, E. Vogel, G. Hohlneicher, J. Michl, J. Am. Chem. Soc. 113 (1991) 5511.
[19] A. Gorski, E. Vogel, J.L. Sessler, J. Waluk, J. Phys. Chem., in press.
[20] M.J. Frisch et al., GAUSSIAN 98, Revision A.6, Gaussian, Inc., Pittsburgh, PA, 1998.
[21] J.E. Ridley, M.Z. Zerner, Theor. Chim. Acta 32 (1973) 111.
[22] M.J.S. Dewar, E.G.E.F. Zoeblisch, Healy, J.J.P. Stewart, J. Am. Chem. Soc. 107 (1985) 3902.
[23] J.J.P. Stewart, J. Comput. Chem. 10 (1989) 209,221.
[24] D. Bremm, G. Hohlneicher, J. Mol. Struct. 480–481 (1999) 591.
[25] P. Borowicz, M. Gil, J. Dobkowski, E. Vogel, J. Waluk, in preparation.
[26] (a) C. Djerassi, Y. Lu, A. Waleh, A.Y.L. Shu, R.A. Goldbeck, L.A. Kehres, C.W. Crandell, A.G.H. Wee, A. Knierzinger, R. Gaete-Holmes, G.H. Loew, P.S. Clezy, E. Bunneberg, J. Am. Chem. Soc. 106 (1984) 4241;
(b) R.A. Goldbeck, B.R. Tolf, A.G.H. Wee, A.Y.L. Shu, R. Records, E. Bunnenberg, C. Djerassi, J. Am. Chem. Soc. 108 (1986) 6449.
[27] (a) M. Gouterman, J. Mol. Spectrosc. 6 (1961) 138;
(b) M. Gouterman, G.H. Wagniere, L.C. Snyder, J. Mol. Spectrosc. 11 (1963) 108.
[28] J. Dobkowski, V. Galievsky, A. Starukhin, E. Vogel, J. Waluk, J. Phys. Chem. A 102 (1998) 4996.
[29] A. Gorski, B. Lament, J.M. Davis, J. Sessler, J. Waluk, J. Phys. Chem. A 105 (2001) 4992.
[30] (a) D. Sundholm, Chem. Phys. Lett. 317 (2000) 392;
(b) J. Hasegawa, Y. Ozeki, K. Ohkawa, M. Hada, H. Nakatsuji, J. Phys. Chem. B 102 (1998) 1320;
(c) J. Hasegawa, M. Hada, M. Nonoguchi, H. Nakatsuji, Chem. Phys. Lett. 250 (1996) 159;

(d) S.R. Gwaltney, R.J. Bartlett, J. Chem. Phys. 108 (1998) 6790;
(e) S. Tretiak, V. Chernyak, S. Mukamel, Chem. Phys. Lett. 297 (1998) 357;
(f) M. Rubio, B.O. Roos, L. Serrano-Andrés, M. Merchán, J. Chem. Phys. 110 (1999) 7202;
(g) L. Serrano-Andrés, M. Merchán, M. Rubio, B.O. Roos, Chem. Phys. Lett. 295 (1998) 195.